멤브레인(Membrane Journal)
Vol. 34 No. 2 April 2024, 154-162

Print ISSN: 1226-0088
Online ISSN: 2288-7253
DOI: https://doi.org/10.14579/MEMBRANE_JOURNAL.2024.34.2.154

셀룰로오스 나노 결정을 도입한 폴리아릴렌 피페리디늄 음이온 교환 복합매질분리막

심 다 혜*·박 현 정*·최 영 우*·박 정 태**·이 재 훈*,†

*한국에너지기술연구원 수소연구단, **연세대학교 디스플레이융합공학과
(2024년 3월 28일 접수, 2024년 4월 12일 수정, 2024년 4월 16일 채택)

Cellulose Nanocrystals Incorporated Poly(arylene piperidinium) Anion Exchange Mixed Matrix Membranes

Da Hye Sim*, Young Park*, Young-Woo Choi*, Jung Tae Park, and Jae Hun Lee*,†**

*Hydrogen Research Department, Korea Institute of Energy Research, Daejeon 34129, Republic of Korea
**Department of Integrated Display Engineering, Yonsei University, Seoul 03722, Republic of Korea
(Received March 28, 2024, Revised April 12, 2024, Accepted April 16, 2024)

요 약: 음이온 교환막은 수전해 시스템에서 매우 중요한 역할을 하며, 생성된 수소와 산소 기체를 물리적으로 분리할 뿐만 아니라 전극 사이에서 수산화 이온의 선택적인 전달을 용이하게 한다. 음이온 교환막에 요구되는 특성은 수산화 이온에 대한 높은 전도도와 알칼리 환경에서의 화학적/기계적 안정성 등이 있다. 본 연구에서는 셀룰로오스 나노 크리스탈이 포함된 poly(terphenyl piperidinium) (qPTP/CNC) 복합매질분리막을 제조하였다. 고분자 매질로 사용된 poly(terphenyl piperidinium)은 super-acid 중합법을 통해 제조되었으며 이온전도성과 알칼라인 내구성이 뛰어난 소재로 알려져 있다. qPTP/CNC 분리막의 구조는 고분자와 나노 입자 계면의 공극이나 큰 응집체가 없는 조밀하고 균일한 형태를 나타냈다. CNC 나노 입자가 2 wt% 첨가된 qPTP/CNC 분리막은 높은 이온교환용량(1.90 mmol/g)과 낮은 함수율(9.09%) 및 팽윤도(5.56%)를 보였다. 또한, 복합막은 수전해 작동 환경인 50°C 1 M KOH에서 상용 FAA-3-50 분리막에 비해 월등히 낮은 저항과 우수한 알칼라인 내구성(384시간)을 달성했다. 이러한 결과는 친수성 첨가제인 CNC가 음이온 교환막의 이온 전도 특성과 알칼라인 내구성 향상에 기여할 수 있음을 보고하였다.

Abstract: Anion exchange membranes (AEMs) are essential components in water electrolysis systems, serving to physically separate the generated hydrogen and oxygen gases while enabling the selective transport of hydroxide ions between electrodes. Key characteristics sought in AEMs include high ion conductivity and robust chemical and mechanical stability in alkaline. In this study, quaternized Poly(terphenyl piperidinium)/cellulose nanocrystals (qPTP/CNC) mixed matrix membrane was fabricated. The polymer matrix, PTP, was synthesized via super-acid polymerization, known for its excellent ion conductivity and alkaline durability. The qPTP/CNC membrane showed a dense and uniform morphology without significant voids or large aggregates at the polymer-nanoparticle interface. The qPTP/CNC membrane containing 2 wt% CNC demonstrated a high ion exchange capacity of 1.90 mmol/g, coupled with low water uptake (9.09%) and swelling ratio (5.56%). Additionally, the qPTP/CNC membrane showed significantly lower resistance and superior alkaline stability (384 hours at 50°C in 1 M KOH) compared to the commercial FAA-3-50 membrane. These results highlight the potential of hydrophilic additive CNC in enhancing ion conductivity and alkaline durability of ion exchange membranes.

Keywords: *anion exchange membrane, poly(arylene piperidine), cellulose nanocrystal, hydrophilic additive*

†Corresponding author(e-mail: jhlee@kier.re.kr; http://orcid.org/0000-0002-0659-7456)

1. Introduction

Hydrogen has been utilized as a carrier for power-to-gas to harness renewable energy. Water electrolysis splits water into oxygen and hydrogen, providing a method for producing green hydrogen without carbon emissions. Water electrolysis can be classified into three types: alkaline water electrolysis (AWE), proton exchange membrane water electrolysis (PEMWE), and anion exchange membrane water electrolysis (AEMWE). AEMWE, which combines the advantages of AWE and PEMWE, has been receiving attention. AEMWE can be performed in alkaline conditions using platinum group metal-free (PGM-free) electrocatalysts, similar to AWE. Additionally, it generates high-purity hydrogen due to the membrane separator, similar to PEMWE[1-4]. In alkaline conditions, the OH^- is provided in the cathode reaction and needs to be transported through the membrane to the catalyst sites in the anode electrode[5]. The electrochemical water splitting reactions in alkaline media are as follows,

$$\begin{aligned} &\text{anode: } 4OH^- \rightarrow O_2 + 2H_2O + 4e^- \\ &\text{cathode: } 4H_2O + 4e^- \rightarrow 2H_2 + 4OH^- \\ &\text{overall: } 2H_2O \rightarrow 2H_2 + O_2 \end{aligned} \quad (1)$$

An anion exchange membrane (AEM) is a fundamental component of AEMWE, designed to prevent gas permeation while facilitating ion exchange for hydrogen production. Poly(aryl ether)-based AEMs have been investigated to meet demanding performance criteria such as high ionic conductivity, mechanical strength, and alkaline stability[6]. However, the presence of ether groups in the polymer backbone can lead to degradation under alkaline conditions due to nucleophilic substitution and Hofmann elimination by attack from hydroxide ions, affecting both the backbone and cationic groups. As a result, ether-free backbones with high chemical stability, such as polynorbornene[7], polystyrene[8], and polyarylene[9] have been proposed in recent years. Poly(arylene piperidinium)s feature ether-free backbones along with heterocyclic ammonium groups. When the hydrophilic and hydrophobic segments dissociate in water, hydroxide ions can be transported into the hydrophilic pathways via Grotthuss and vehicular mechanisms[10]. However, AEMWE still faces limitations such as lower current density resulting from lower hydroxide conductivity compared to protons, as well as challenges related to long-term stability and the trade-off between conductivity and dimensional stability. Various strategies have been proposed to address these issues, including grafting side chains or utilizing crosslinkers[11,12].

Cellulose is a linear polysaccharide comprising thousands of β-1,4-linked D-glucose units. Its architecture consists of crystalline and amorphous domains, which vary depending on the polymerization degree and chain length. Cellulose exhibits strong hydrogen bonds, contributing to its stability and solubility in only specific solvents. Through processes such as acid hydrolysis and mechanical treatment, cellulose can be classified into microcrystalline cellulose (MCC), cellulose nanocrystals (CNC), cellulose nanofibers (CNF), and bacterial nanocellulose (BC). CNCs are needle-like nanoparticles with sizes less than 100 nm. The advantages of cellulose include its hydrophilicity, low cost, biodegradability, and superior mechanical and thermal properties. Therefore, AEMs containing cellulose polymers have been reported in various literatures[13-15].

In this study, we investigate the effect of hydrophilic additives CNCs on AEMs for water electrolysis. The hydroxide ion conductivity and mechanical properties can be influenced by increasing the ion exchange capacity (IEC). However, higher IEC values may render AEMs more susceptible to attack by hydroxide ions due to their increased hydrophilicity. Therefore, a strategic balance between high IEC and low water uptake can be achieved through the formation of appropriate water channels by incorporating hydrophilic additives [16,17]. Quaternized poly(2,4,6-trimethyl-1,3-phenylene) (PTP) was selected as the polymer matrix, as it is

commonly studied in AEM research. Mixed matrix membranes were prepared by solution casting method with incorporation of cellulose nanocrystals fillers. To validate the electrochemical properties of the mixed matrix membrane proposed in this study, we utilized the widely used commercial anion exchange membrane FAA-3-50 as the control group. The structure of commercial FAA-3-50 is reported to consist of a poly(phenylene oxide) (PPO) backbone and quaternary ammonium groups.

2. Materials and Methods

2.1. Materials

p-terphenyl (99.5%), *N*-Methyl-4-piperidone (m-pip, 97%), trifluoromethanesulfonic acid (TFSA, 98%), trifluoroacetic acid (TFA, 99%), methyl iodide (CH_3I, 99%), dichloromethane (DCM, 99%), *N*-methyl-2-pyrrolidone (NMP, 99%), potassium carbonate (K_2CO_3, 99%) were purchased from Sigma-Aldrich (St. Louis, MO, USA). The dimethyl sulfoxide (DMSO, 99%) was purchased from Duksan Chemicals (Ansan, Korea). Cellulose nanocrystals (CNC-DS-SD) were purchased from Cellulose Lab Inc. (Fredericton, Canada).

2.2. Synthesis of quaternized Poly(terphenyl piperidinium)

p-terphenyl (4.96 g) and m-pip (3.06 mL) were dissolved in DCM (20 mL) in a 250 mL round-bottom flask with mechanical stirring. After homogeneous dissolving, reaction was carried out at 0°C in ice bath. The TFA (1.77 mL) and TFSA (15 mL) were added dropwise into the reaction for 3 hours. The solution became viscous and precipitated in DI water. The fibrous polymer obtained and washed several times with DI water. Thereafter, resultant polymer was filtered and dried in oven at 80°C for overnight to obtain PTP.

Quaternization of PTP was achieved by Menshutkin reaction. The PTP (2 g) polymer was dissolved in mixed solvent including DMSO (20 mL) and NMP (40 mL). To remove remaining acid residue, K_2CO_3 (0.42 g) was added. CH_3I (1.91 mL) was added to the solution under dark conditions. The solution was kept at 80°C for 8 h. After cooling, the brown product was precipitated in diethyl ether. It was filtered and washed with diethyl ether and DI water. At last, the product was dried in oven at 80°C for 24 h to obtain quaternized PTP.

2.3. Membrane preparation

qPTP (0.2 g) was completely dissolved in DMSO (6 mL). Meanwhile, CNC (0.04 g, 2 wt%) was dispersed in DMSO (2 mL) with ultrasonicated and added into qPTP solution. The reason for selecting 2 wt% CNC is that when more than 5 wt% of CNC was added, visible agglomeration of CNC particles was observed, leading to a deterioration in the mechanical properties of the membrane. Additionally, literature reports have shown that around 2 wt% of nanoparticle addition is optimal for observing the effects of particles[18]. The mixture was vigorously stirred at 80°C for overnight. The whole solution was cast onto a glass plate and dried at 80°C for 24 h to form a composite membrane of uniform thickness. After that, the membrane was washed with DI water. and immersed in 1 M KOH solution at room temperature for 24 h to exchange the anion. Subsequently, the membrane was thoroughly washed with DI water.

2.4. Characterization

The Fourier transform infrared spectroscopy (FT-IR, Spectrum 100, PerkinElmer, USA) was used to analyse the chemical bonds of the polymers. 1H-NMR was also performed to confirm the chemical structure and ratio of monomers. The morphology of the composite membrane was characterized using field emission scanning electron microscopy (FE-SEM). To determine the impact of the polymer backbone structure on the characteristics of AEMs, tests were performed on the electrochemical characteristics of each AEMs, including IEC, water uptake (WU), swelling ratio (SR), and alkaline stability test.

The IEC of the AEMs was determined by an acid-base titration method, which was defined as the

mole number of ionic groups per unit mass of dry membrane. To replace all OH^- ions with Cl^- ions, a dry membrane was soaked in 0.05 M HCl solution for 24 h at room temperature. Following, the titration was carried out with a standard 0.05 M NaOH solution using phenolphthalein as an end-point indicator. The IEC was calculated based on the following equations

$$IEC(mmol/g) = \frac{C_{HCl}V_{HCl} - C_{NaOH}V_{NaOH}}{m_{dry}} \quad (2)$$

where C_{HCl} and C_{NaOH} are the molar concentration (M) of HCl and NaOH solution, respectively. V_{HCl} and V_{NaOH} are the volume (mL) of HCl and NaOH solution respectively. m_{dry} is the mass (g) of the dry AEM.

For WU and SR, the OH^- form membranes were immersed in DI water at 30°C and 80°C each other for 24 h, and then they were removed from the DI water quickly. Their mass (m_{wet}) and length (L_{wet}) were recorded. The membranes were dried at 60 for 24 h with the mass (m_{dry}) and length (L_{dry}) measured. The WU and SR can be calculated as follow as

$$WU = \frac{m_{wet} - m_{dry}}{m_{dry}} \times 100\% \quad (3)$$

$$SR = \frac{L_{wet} - L_{dry}}{L_{dry}} \times 100\% \quad (4)$$

The area resistance (AR) is measured according to the equation

$$AR(\Omega cm^2) = Resistance \times Area \quad (5)$$

To determine alkaline stability, The AR was measured using an inductance-capacitance-resistance (LCR) meter (LCR-6100, QWINSTEK, South Korea) at a frequency of 10 kHz. The qPTP/CNC_2 wt% and commercial FAA-3-50 (FuMa-Tech CO., Germany) membranes were pretreated in 1 M KOH at 50°C, and then the area resistances were measured for 384 h with an area of 0.785 cm^2.

3. Results and Discussion

PTP was successfully synthesized via super-acid catalyzed Friedel-Crafts polycondensation between p-terphenyl and N-methyl-4-piperidinone (Scheme 1) As the reaction progressed, the viscosity of the reactant gradually increased, resulting in a dark blue solution. After precipitation in DI water, a white fibrous solid was obtained. PTP is soluble in polar solvents such as NMP, and after the quaternization process, qPTP becomes soluble in both DMSO and NMP. Fig. 1 illustrates the preparation procedure of the qPTP/CNC mixed matrix membrane. The CNC-dispersed solution was added to the polymer solution after sonication to enhance dispersity and miscibility between nanoparticles and polymer chains. The qPTP/CNC mixed matrix membrane was fabricated using the solution

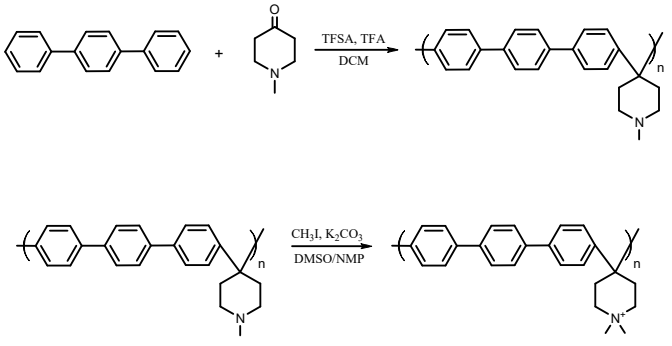

Scheme 1. Chemical structure of PTP and qPTP.

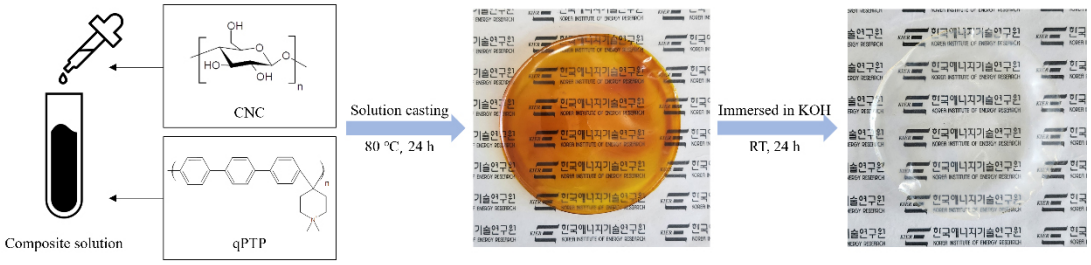

Fig. 1. Preparation of the qPTP/CNC mixed matrix membrane.

casting method on a glass dish. Subsequently, the membranes were immersed in 1 M KOH to convert the counter-ions from iodide form to hydroxide form. As the counter ion changed, the color of the membrane transitioned from brown to transparent. The prepared membrane exhibited flexibility and strong strength.

Fig. 2 depicts the FT-IR spectra of PTP, qPTP, and the qPTP/CNC 2 wt% membrane. The absorption bands at 3027 and 2960 cm^{-1} in PTP and qPTP correspond to aromatic and aliphatic C-H bonds, respectively. The broad band observed at 3600-3300 cm^{-1} and 1621 cm^{-1} corresponds to O-H bonding of adsorbed water. Additionally, the band observed at 1467 cm^{-1} in the IR spectrum of qPTP is associated with $C\text{-}N^{+}$ bonds, indicating the successful quaternization reaction. Furthermore, the bands observed at 1161 cm^{-1}, 1105 cm^{-1}, and 1026 cm^{-1} in the spectra of the qPTP/CNC membrane are assigned to C-O-C asymmetric stretching, C-O vibration, and stretching bonding of the cellulose nanocrystals, respectively[19]. This result suggests that CNC nanoparticles are physically dispersed in the qPTP matrix with weak interactions.

Analysis of the chemical structure and synthesis of qPTP was investigated using ^{1}H-NMR spectra of qPTP shown in Fig. 3. The characteristic peaks at 7.41~7.85 ppm ($H_{d,e}$) can be attributed to the aromatic protons of the terphenyl groups, while the peaks at 3.54 to 2.68 ppm ($H_{a,b,c}$) represent proton peaks of piperidine and methyl groups. Additionally, the splitting of the H_a and H_b peaks in the spectrum could be attributed to the N-protonation of the piperidine ring.[20]. The strong peak at 3.44 ppm was attributed to the effect of water, which could be mitigated by adding small amounts of

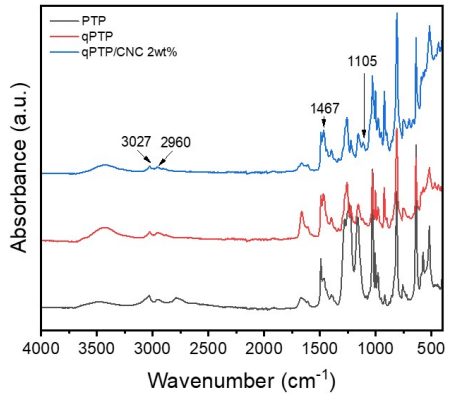

Fig. 2. FT-IR spectra of PTP, qPTP, and qPTP/CNC_2 wt%.

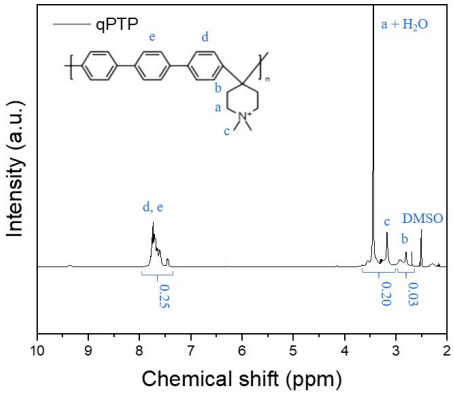

Fig. 3. ^{1}H-NMR spectra of qPTP.

d1-TFA. The addition of small quantities of d1-TFA results in a downfield displacement of the water signal[21]. Additionally, the ratio between the two monomers of a random copolymer can be determined by comparing the integral areas of their respective peaks. The integral area of terphenyl groups was found to be almost similar to that of piperidine groups, indicating

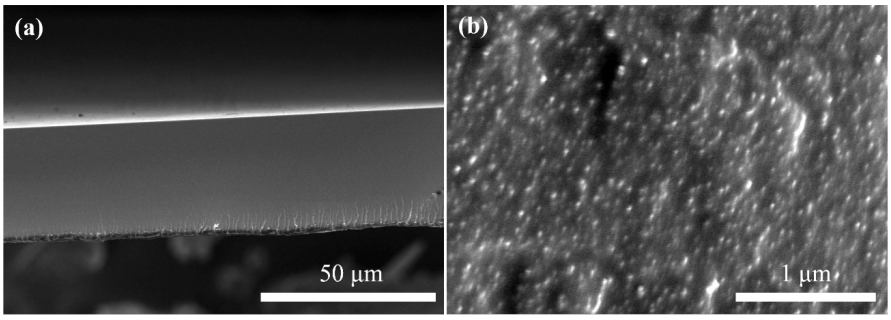

Fig. 4. FE-SEM images of the qPTP/CNC membrane with (a) low and (b) high magnification.

that the two monomers reacted well at a ratio of 1:1. Thus, the ^{1}H NMR and FT-IR spectra confirm the successful synthesis of quaternized PTP.

CNC nanofillers possess a large surface area with the polymer matrix, enabling them to generate a maximum reinforcing effect even with a low loading amount[22]. The homogeneous dispersion of reinforcement in a polymer matrix is a crucial requirement for effectively improving the mechanical properties. Therefore, compatibility is important to achieve the desired improvement in properties, and morphology is closely related to compatibility. Fracture morphologies of the prepared membranes were examined using FE-SEM. Fig. 4 shows the qPTP/CNC membrane at different magnifications. The membrane appears dense and uniform morphology, effectively facilitating ion transporting and hindering gas permeation. Upon closer inspection in Fig. 4b, the surface of the qPTP/CNC membrane is composed of regularly distributed particles with diameters ranging from 40 to 50 nm. This suggests that the CNC surfaces with hydroxyl groups exhibit good compatibility with qPTP.

Water uptake is typically one of the important parameters that increase ionic conductivity. Quaternary ammonium groups are hydrated in alkaline conditions, enabling them to transport hydroxide ions. However, this hydration also leads to dimensional swelling, resulting in a decrease in dimensional stability and mechanical properties. The cell performance in AEMWE can be influenced by the dimensional stability of AEMs. Therefore, it is crucial to secure both ionic conductivity and dimensional stability by maintaining a high IEC while decreasing water uptake and swelling ratio[23].

Table 1. SR, WA, and IEC of the qPTP and qPTP/CNC_2 wt% Membranes

	WU (%)		SR (%)		IEC
	30°C	80°C	30°C	80°C	(mmol/g)
qPTP	27.02	35.16	10	12.5	1.69
qPTP/CNC 2 wt%	9.09	13.64	5.56	8.33	1.90

Table 1 presents the water uptake (WU), swelling ratio (SR), and ionic exchange capacity (IEC) to confirm dimensional stability. The WU and SR of all AEMs show an increase as the temperature rises from 25°C to 80°C. This phenomenon occurs because the free volume, which increases with rising temperature, can accommodate more water[24]. Moreover, the dimensional stability of the membrane remains good even at increasing temperatures. Surprisingly, despite the use of CNCs as hydrophilic filler, the water uptake of the membrane decreased, contrary to expectations of increased hydration and membrane swelling. This result may be attributed to the strong interaction between CNCs and quaternized PTP molecules. The increase in IEC observed after the addition of 2 wt% CNC suggests that the hydrophilic functional groups of CNC contributed to the formation of water channels and enhancement of ionic conductivity. Consequently, the composite membrane maintained a high IEC while exhibiting good dimensional stability.

The low resistance and excellent alkaline stability of AEMs is a crucial parameter for cost-efficiency and

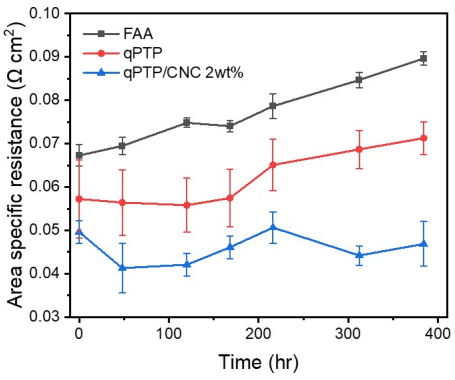

Fig. 5. AR of FAA, qPTP and qPTP/CNC_2 wt% membranes.

long-term operation in AEMWE, as highlighted in numerous studies[25-27]. To evaluate resistance and chemical stability in alkaline conditions simultaneously, the area resistance (AR) of the qPTP and qPTP/CNC 2 wt% were measured and compared with a commercial anion exchange membrane (FAA-3-50) over a period of 384 hours. AR measurement was conducted at 50°C under 1 M KOH condition to mimic AEWWE operating environment. Fig. 5 illustrates that the qPTP/CNC 2 wt% exhibits a lower resistance value compared to the pristine qPTP and commercial FAA-3-50, indicating excellent hydroxide ion conductivity. Furthermore, the AR trend of the qPTP/CNC 2 wt% remained consistent between the initial and terminal states. After approximately 400 hours, the AR of the FAA-3-50 noticeably increased by 33% compared to its initial state. In contrast, qPTP/CNC 2 wt% maintained its initial resistance value, confirming their excellent alkaline stability.

4. Conclusions

In conclusion, we investigated the effect of CNC as a hydrophilic additive on polyarylene-based mixed matrix AEMs. It was anticipated that AEMs with appropriate CNC content would establish a hydrophilic region and expand the ion transfer pathway. Accordingly, PTP was synthesized via super-acid catalyzed polycondensation, and successful synthesis was confirmed through FT-IR and ^{1}H-NMR analyses. FE-SEM analysis revealed well-distributed CNC particles within the qPTP matrix without large agglomerate. Consequently, the qPTP/CNC 2 wt% exhibited excellent physicochemical properties, with a high IEC of 1.9 mmol/g yet low WU and SR of 13.64% and 8.33%, respectively, at 80°C. In the AEWWE operating environment (50°C under 1 M KOH), qPTP/CNC 2 wt% exhibited a significantly lower AR value compared to commercial FAA-3-50, suggesting the potential to enhance water electrolysis efficiency using qPTP/CNC 2 wt%. Also, the good alkaline stability of qPTP/CNC 2 wt% for 384 hours at same condition. These findings demonstrate that incorporating hydrophilic CNC additives improves the mechanical and electrochemical properties of AEMs for water electrolysis through uniform distribution and the formation of proper ion-conducting channels.

Acknowledgements

This research was supported by the Ministry of Trade, Industry, and Energy (MOTIE, Korea) (20218 520040040 and 20203030040030).

Reference

1. K. F. L. Hagesteijn, S. Jiang, and B. P. Ladewig, “A review of the synthesis and characterization of anion exchange membranes”, *J. Mater. Sci.*, **53**, 11131 (2018).
2. H. A. Miller, K. Bouzek, J. Hnat, S. Loos, C. I. Bernäcker, T. Weißgärber, L. Röntzsch, and J. Meier-Haack, “Green hydrogen from anion exchange membrane water electrolysis: A review of recent developments in critical materials and operating conditions”, *Sustain. Energy Fuels*, **4**, 2114 (2020).
3. S. A. Lee, J. Kim, K. C. Kwon, S. H. Park, and H. W. Jang, “Anion exchange membrane water electrolysis for sustainable large-scale hydrogen

production", *Carbon Neutralization*, **1**, 26 (2022).
4. I. Vincent and D. Bessarabov, "Low cost hydrogen production by anion exchange membrane electrolysis: A review", *Renew. Sustain. Energy Rev.*, **81**, 1690 (2018).
5. N. Du, C. Roy, R. Peach, M. Turnbull, S. Thiele, and C. Bock, "Anion-exchange membrane water electrolyzers", *Chem. Rev.*, **122**, 11830 (2022).
6. D. Pan, T. H. Pham, and P. Jannasch, "Poly(arylene piperidine) anion exchange membranes with tunable N-alicyclic quaternary ammonium side chains", *ACS Appl. Energy Mater.*, **4**, 11652 (2021).
7. M. Mandal, G. Huang, N. U. Hassan, W. E. Mustain, and P. A. Kohl, "Poly(norbornene) anion conductive membranes: Homopolymer, block copolymer and random copolymer properties and performance", *J. Mater. Chem. A*, **8**, 17568 (2020).
8. N. Yu, J. Dong, H. Li, T. Wang, and J. Yang, "Improving the performance of quaternized SEBS based anion exchange membranes by adjusting the functional group and side chain structure", *Eur. Polym. J.*, **154**, 110528 (2021).
9. T. H. Pham, J. S. Olsson, and P. Jannasch, "Poly(arylene alkylene)s with pendant N-spirocyclic quaternary ammonium cations for anion exchange membranes", *J. Mater. Chem. A*, **6**, 16537 (2018).
10. R. Vinodh, S. S. Kalanur, S. K. Natarajan, and B. G. Pollet, "Recent advancements of polymeric membranes in anion exchange membrane water electrolyzer (AEMWE): A critical review", *Polymers*, **15**, 2144 (2023).
11. L. Liu, L. Bai, Z. Liu, S. Miao, J. Pan, L. Shen, Y. Shi, and N. Li, "Side-chain structural engineering on poly(terphenyl piperidinium) anion exchange membrane for water electrolysers", *J. Membr. Sci.*, **665**, 121135 (2023).
12. J. S. Olsson, T. H. Pham, and P. Jannasch, "Tuning poly(arylene piperidinium) anion-exchange membranes by copolymerization, partial quaternization and crosslinking", *J. Membr. Sci.*, **578**, 183 (2019).
13. S. Thangarasu, T. H. Oh, "Recent developments on bioinspired cellulose containing polymer nanocomposite cation and anion exchange membranes for fuel cells (PEMFC and AFC)", *Polymers*, **14**, 5248 (2022).
14. X. Cheng, J. Wang, Y. Liao, C. Li, and Z. Wei, "Enhanced conductivity of anion-exchange membrane by incorporation of quaternized cellulose nanocrystal", *ACS Appl. Mater. Interfaces*, **10**, 23774 (2018).
15. G. Das, B. J. Park, J. Kim, D. Kang, and H. H. Yoon, "Quaternized cellulose and graphene oxide crosslinked polyphenylene oxide based anion exchange membrane", *Sci. Rep.*, **9**, 9572 (2019).
16. M. Mandal, "Recent advancement on anion exchange membranes for fuel cell and water electrolysis", *ChemElectroChem*, **8**, 36 (2021).
17. W. Tang, T. Mu, X. Che, J. Dong, and J. Yang, "Highly selective anion exchange membrane based on quaternized poly(triphenyl piperidine) for the vanadium redox flow battery", *ACS Sustain. Chem. Eng.*, **9**, 14297 (2021).
18. R. Vinodh and D. Sangeetha, "Comparative study of composite membranes from nano-matal-oxide-incorporated polymer electrolytes for direct methanol alkaline membrane fuel cells", *J. Appl. Polym. Sci.*, **128**, 1930 (2013).
19. Z. Kassab, I. Kassem, H. Hannache, R. Bouhfid, A. E. K. Qaiss, and M. El Achaby, "Tomato plant residue as new renewable source for cellulose production: extraction of cellulose nanocrystals with different surface functionalities", *Cellulose*, **27**, 4287 (2020).
20. J. S. Olsson, T. H. Pham, and P. Jannasch, "Poly(arylene piperidinium) hydroxide ion exchange membranes: synthesis, alkaline stability, and conductivity", *Adv. Funct. Mater.*, **28**, 1702758 (2018).
21. S. A. Ross and G. Lowe, "Downfield displacement of the NMR signal of water in deuterated dimethylsulfoxide by the addition of deuterated trifluoroacetic acid", *Tetrahedron Lett.*, **41**, 3225 (2000).

22. A. D. de Oliveira and C. A. G. Beatrice, “Polymer nanocomposites with different types of nanofiller”, *Nanocomposites − Recent Evolutions*, p. 103, Intech Open, London, United Kingdom (2018).
23. M. I. Khan, A. N. Mondal, B. Tong, C. Jiang, K. Emmanuel, Z. Yang, L. Wu, and T. Xu, “Development of BPPO-based anion exchange membranes for electrodialysis desalination applications”, *Desalination*, **391**, 61 (2016).
24. J. Zheng, J. Wang, S. Zhang, T. Yuan, and H. Yang, “Synthesis of novel cardo poly(arylene ether sulfone)s with bulky and rigid side chains for direct methanol fuel cells”, *J. Power Sources*, **245**, 1005 (2014).
25. L. Zhu, X. Yu, X. Peng, T. J. Zimudzi, N. Saikia, M.T. Kwasny, S. Song, D. I. Kushner, Z. Fu, G. N. Tew, W. E. Mustain, M. A. Yandrasits, and M. A. Hickner, “Poly(olefin)-based anion exchange membranes prepared using ziegler-natta polymerization”, *Macromolecules*, **52**, 4030 (2019).
26. M. Zeng, X. He, J. Wen, G. Zhang, H. Zhang, H. Feng, Y. Qian, and M. Li, “*N*-Methylquinuclidinium-based anion exchange membrane with ultrahigh alkaline stability”, *Adv. Mater.*, **35**, 2306675 (2023).
27. Y. Ma, C. Hu, G. Yi, Z. Jiang, X. Su, Q. Liu, J. Y. Lee, S. Y. Lee, Y. M. Lee, and Q. Zhang, “Durable multiblock poly(biphenyl alkylene) anion exchange membranes with microphase separation for hydrogen energy conversion”, *Angew. Chem. Int. Ed.*, 62, e202311509 (2023).